APPLIED ORGANOMETALLIC CHEMISTRY
Appl. Organometal. Chem. 2004; **18**: 506–513
Published online in Wiley InterScience (www.interscience.wiley.com). DOI:10.1002/aoc.753

Superparamagnetic iron oxide particles: contrast media for magnetic resonance imaging†

Rüdiger Lawaczeck[1]*, Michael Menzel[2] and Hubertus Pietsch[1]

[1]Schering AG, Research Laboratories Berlin, Müllerstr. 178, D-13342 Berlin
[2]Federal Institute of Materials Research and Testing (BAM), Richard-Willstätter-Str. 11, D-12489 Berlin

Received 28 October 2003; Accepted 18 February 2004

The mainstream magnetic iron oxide particles used as contrast media for magnetic resonance (MR) imaging are composed of a magnetic iron oxide core surrounded by a dextran or carboxydextran coat. The core size ranges from 2 nm to less than 10 nm, and the hydrodynamic diameter ranges from 20 nm to about 120 nm. The coat prevents aggregation and sedimentation of the particles in aqueous solutions, achieves high biological tolerance, and prevents toxic side effects.

Two kinds of particles are considered: (i) large particles (>30 nm), called superparamagnetic iron oxide particles (SPIOs) for liver imaging; (ii) smaller particles (<30 nm hydrodynamic diameter), called ultrasmall SPIOs (USPIOs), e.g. for MR angiography.

To characterize the particles, Mössbauer spectra are presented for the two particle ensembles. These spectra allow insight into the magnetic coupling, the valency of the iron ions and a rough estimate of the core size to be deduced. On the basis of the concentration dependence of the MR signal intensities, two applications are discussed together with two representative clinical examples.

Future indications for MR diagnostics, e.g. the labeling and tracking of stem cells during stem-cell therapy control, are outlined.

KEYWORDS: superparamagnetic; iron oxide particles; MR imaging; contrast media

INTRODUCTION

Magnetic ferrofluids for pharmaceutical or medical application consist of a stable aqueous dispersion of magnetic iron oxide particles. In the case of ferrofluids for parenteral applications in diagnostic imaging, the particles are constructed of inorganic magnetic cores usually coated by carbohydrate layers to prevent aggregation and sedimentation of the particles and to endow these particles with pharmacological properties to allow parenteral administration. Magnetic particles for oral application can have a different construction plan. In this case it is not necessary to have one single magnetic core surrounded by one individual carbohydrate coat. Instead, one net-like carbohydrate layer or protein structure could anchor several magnetic iron oxide cores; rigid coats are also available.

In most cases iron oxide particles were considered. Two of them are ferromagnetic and are of principal importance,[1] i.e. γ-Fe_2O_3 (also known as maghemite) and Fe_3O_4 (known as magnetite). Ferrofluids used for medical purposes are synthesized by wet synthesis, usually starting from the inorganic iron salts, in contrast to synthesis methods where particles of desired size are prepared by milling of separately prepared and larger particles. In a second step, the aqueous solutions of these particles have to be stabilized. Details of the crystal-forming process still await a profound explanation on an atomistic scale; the same holds for the interaction between the iron oxide core and the organic coat.

Magnetic particles are abundant in nature, from bacteria to man, in the form of microcrystals surrounded by layers of organic molecules and proteins. These magnetic particles are thought to serve for navigation in the Earth's magnetic field. They could, next to ferritin, also serve as a biological storage of iron. As reviewed by Häfeli,[2] the name magnetite might originate from Magnesia, a sunken town in Asia Minor, i.e. Modern-day Turkey.

Owing to the complexity of ferrofluids or sols of magnetic particles, a wide arsenal of physical, pharmaceutical and biological techniques is necessary to characterize the particles in question. This investigation process includes electron microscopy, Mössbauer spectroscopy, magnetic susceptibility and relaxivity, X-ray diffraction, laser light scattering and

*Correspondence to: Rüdiger Lawaczeck, Schering AG, Research Laboratories Berlin, Müllerstr. 178, D-13342 Berlin, Germany.
E-mail: ruediger.lawaczeck@schering.de
† For Anne (1951–2004).

size fractionation on the physical side, and pharmacokinetic and pharmacodynamic studies and organ distribution on the biological side. Pharmaceutical stability, ease of synthesis and conformity with the registration laws for parenteralia, i.e. the ability for heat sterilization or a pyrogene-free way of synthesis, are inherent prerequisites to be fulfilled. Last, but not least, a therapeutic or diagnostic benefit has to be proven.

For the mainstream magnetic particles of diagnostic imaging, two acronyms are widely used: superparamagnetic iron oxide (SPIO) particles and ultrasmall superparamagnetic iron oxide (USPIO) particles.

Within the SPIO family, two compounds are registered and approved: one compound goes under the name of Feridex® (Berlex) in the USA or Endorem® (Guerbet) in Europe, and the second is Resovist® (Schering) in Europe and Japan. In both cases the clinical targets are liver and spleen tumors. The particles are of medium size and coated with dextran (Feridex®, Endorem®) or an alkali-treated low molecular weight dextran, called carboxydextran (Resovist®). In addition to the iron oxide particles and the coating material, both drugs contain pharmaceutical auxiliary substances to assure neutral pH or isotonicity with blood. They are manufactured for intravenous (i.v.) administration.

USPIO particles originate from SPIOs and are very similar in composition to the leading compounds, but they are smaller in total diameter, resulting in lower values for the T_2 relaxivities. Initially they were a subset of the SPIOs obtained by size fraction.[3] Today, other methods of fractionation are available or the USPIOs are especially prepared, thus avoiding time-consuming fractionation processes. The differences between SPIO and USPIO are the longer blood half-life of the smaller particles and the lower T_2 relaxivity of the latter. The long blood half-life of 1–2 h versus several minutes for the normal superparamagnetic particles opens up new clinical indications, e.g. magnetic resonance (MR) angiography and the targeting of organs other than spleen, liver or bone marrow, the conventional reticuloendothelial system (RES). Recently, USPIOs with citric acid coating have been developed. These particles have a small hydrodynamic radius due to the small citric acid layer. They are called very small superparamagnetic iron oxide particles (VSOPs), and are under clinical development for the demarcation of coronary arteries.[4,5]

A third clinical target is the gastro-intestinal tract, where oral magnetic particles (OMPs) are available. These are larger magnetic particles prepared in a different way with non-biodegradable coating matrices composed of siloxane or polystyrene. They serve for the demarcation of gastro-intestinal lesions.[6,7]

Besides these magnetic particles which are already registered or in clinical development, there are also a variety of magnetic particles in experimental studies covering both *in vitro* and *in vivo* diagnostics and therapy. Target molecules coupled to monocrystalline iron oxide nanoparticles[8] are considered as one powerful tool for MR molecular imaging of the future.

In the following, a short overview of the synthesis, physical characterization, and physiological behavior is presented. The contrasting efficiency in MR imaging will be explained and verified by two characteristic examples. The focus will be on clinically available magnetic iron oxide particles for parenteral application.

SYNTHESIS OF SPIOs

Magnetic iron oxide particles for pharmaceutical use are usually prepared by an alkaline precipitation of solutions containing iron(II) and iron(III) salts.[9,10] The alkaline precipitation reaction is performed in the presence of the coating substances, i.e. dextrans. Hasegawa and Hokkoku[11] proposed a typical manufacturing method for magnetic iron oxide particles coated with alkali-treated dextran. The method has been improved and technically modified. Today, a number of magnetic iron oxide particle types are known. The modifications made concerning the initial method relate to the coating materials, the iron oxide core size, the valency of iron ions and the formulation or additives to the final drug product. The modifications have resulted in a wide spectrum of magnetic particles, given the particles various physical and physiological properties and widened their use.

In the Hasegawa and Hokkoku synthesis method the sol is prepared by mixing an aqueous solution of the ferric and ferrous salts in suitable ratio and in the presence of the coating material with an aqueous solution of an alkaline substance such as sodium hydroxide. On separating the precipitate from the reaction solution, the pH of the solution is neutralized by the addition of hydrochloric acid. In subsequent steps the solution can be purified by dialysis or ultra-filtration.

Weissleder and coworkers[3,11] pioneered the use of small superparamagnetic particles. The USPIOs were obtained by size fractionation using size-exclusion gel chromatography. Today, this fractionation repertoire has been widened by several other methods. Various factors have an influence on the final sol of magnetic particles, and the methods of preparation are numerously modified. Many coating materials have been proposed, such as dextran,[13] starch, arabinogalactan,[15] glycosaminoglycan,[16] carboxydextran.[17]

For target-specific magnetic iron oxide particles a target-specific molecule must be attached to the coat. One way of performing this is by covalently coupling the target molecules to the dextran coat via the periodate oxidation of hydroxyl groups of the glucose units.[18,19] Cerdan *et al*.[20] directly covered plain iron oxides with monoclonal antibodies and achieved a targeting of the receptor molecules. The coupling methods have been refined; today, in a modular building block principle, a variety of target molecules can be attached to the coat of the iron oxide particles. It has turned out to be advantageous to first crosslink the coating molecules before the target molecules are bound.[21]

CHARACTERIZATION OF THE SOL OF MAGNETIC IRON OXIDE PARTICLES

For reproducible production and quality control the particles must be characterized according to their composition and physical measures. Next to the iron and carbohydrate analysis, a variety of physical methods have been developed to characterize the particles. The particles are composed of an iron oxide core coated with a carbohydrate coat, usually dextran or carboxydextran. The methods can be grouped into those determining qualities of the core and those determining qualities of the overall particle in solution.

Core properties

The core is electron dense and is thus visible in electron micrographs. From these micrographs the core dimension can be deduced. The crystal structure can be verified from X-ray diffraction patterns, where γ-Fe_2O_3 and Fe_3O_4 show similar reflections. From the width of the reflection lines the core dimensions can also be calculated under certain assumptions (Scherrer formula). Mössbauer spectra (a resonant absorption of nuclear gamma radiation, e.g. of the non-radioactive ^{57}Fe isotopes) give information on the magnetic coupling, on the valence state of the iron ions and also on the size of the core. Fig. 1 shows Mössbauer spectra of lyophilized SPIO and USPIO samples at room temperature.

In the mixed-valent iron oxide magnetite (Fe_3O_4) the Fe^{3+} is evenly distributed over the tetrahedral and octahedral sites, whereas the Fe^{2+} occupies only the octahedral lattice sites. Owing to the strong ferromagnetic coupling of the antiparallel type between the ions occupying two different lattice sites, the magnetic component of the Fe^{3+} ions cancels and the residual magnetism originates from the Fe^{2+} ions; this is called ferrimagnetism. Fe_3O_4 can be oxidized to γ-Fe_2O_3 without major change of the magnetic properties. In γ-Fe_2O_3 the trivalent iron is randomly distributed over the octahedral and tetrahedral lattice sites.

The Mössbauer spectrum of the larger particles, the SPIOs, shows a number of sextets reflecting the ferromagnetic coupling, paramagnetic doublets and the transition from the ferromagnetic to the paramagnetic coupling. For the mathematical fitting, four sextets, two doublets and one transition spectrum were introduced. The calculation of the sextets was performed with four classes of core sizes ranging from 7 to 15 nm according to Prene *et al.*[22] The decrease in size of the smaller particles, the USPIOs, results in a loss of the ferromagnetic coupling in parallel with an increase of the quadrupole-coupled paramagnetic doublets. In both cases, SPIO and USPIO, the isomer shift values are consistent with a low Fe^{2+} content, favoring the γ-Fe_2O_3 structure.

Particles in solution

Hydrodynamic radius

Apart from magnetic properties, which have a fundamental influence on the magnetic resonance imaging parameters, the hydrodynamic size or radius is of principal importance since it determines the physiological pathway or biodistribution. Also, the coat may have an influence on physiological uptake mechanisms. The hydrodynamic size is deduced from the diffusion coefficient and measured by dynamic light scattering. Polydispersity and the weighting average enter into the calculations of the hydrodynamic radius from these measurements. The hydrodynamic size can also be obtained from size-exclusion chromatography. Since the weighting is different, the results of both methods do not necessarily coincide.

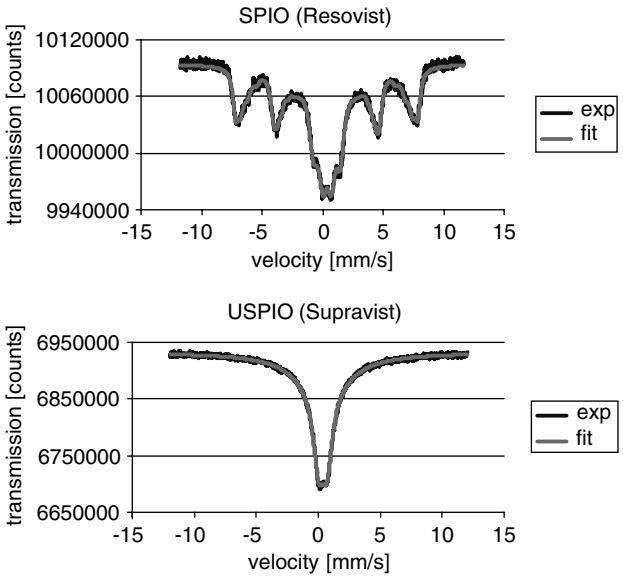

Figure 1. Mössbauer spectra of SPIO and USPIO particles: transmission versus Mössbauer velocity at room temperature. (a) SPIO experimental spectra were fitted by four sextets reflecting the ferromagnetic coupling (γ-Fe_2O_3) and two quadrupole-coupled doublets as well as a broad transition between the sextet and the doublet. Instead of a continuous core-size distribution, sextets corresponding to four classes from 7 to 15 nm were used for the mathematical fitting procedure. (b) USPIO experimental spectra were fitted by two quadrupole-coupled doublets and one broad transition between a ferromagnetic sextet and a paramagnetic doublet. The isomer shifts are between 0.33 and 0.37 for the sextets and between 0.37 and 0.38 mm s^{-1} for the doublets. respectively.

Magnetic behavior, magnetization

Material in a magnetic field experiences a magnetization. For diamagnetic material the induced magnetization is very small and opposite to the direction of the magnetic field. Paramagnetic molecules and ferromagnetic particles align their magnetic dipoles in the field direction counterbalanced by thermal fluctuations. Measurements of the magnetization as a function of the applied magnetic field allow the determination of magnetic properties (magnetic susceptibility and saturation magnetization).

For SPIOs and USPIOs the magnetization increases steeply with increasing magnetic field and reaches a plateau. By decreasing the magnetic field the magnetization decreases on the same curve, passes zero and decreases to negative values with increasing negative field strength. The negative or positive plateau-values correspond to a state where all magnetization vectors are aligned parallel to the applied field. These values serve to characterize the magnetic particles (saturation magnetization).

For ferromagnetic particles in solution with sizes less than the single domain size, thermal agitation of the whole particle leads to an overall tumbling of the particles (Brown motion). In addition, the thermal fluctuations of the individual ions around the equilibrium lattice sites counteract that the direction of the magnetization is fixed in one direction. Instead, it can jump randomly from one to another direction (Néel relaxation). Particles with these magnetic properties are called superparamagnetic. Solutions of these particles do not show remanence or hysteresis. Usually, superparamagnetic behavior is observed for particles with crystal or core diameters less than 30 nm.

Relaxivities

For a given pulse sequence the MR imaging (MRI) signal intensity is determined by three parameters: the local proton density (water and/or fat protons) and the two magnetic relaxation times, T_1 and T_2. T_1, also called the longitudinal or spin–lattice relaxation time, is a measure of how fast magnetic energy is released or taken up (to/from the lattice). If material is suddenly exposed to a magnetic field the macroscopic magnetization, which is the vector sum of the individual atomic moments of the material in the field, will be built up with the characteristic time T_1. T_2, the transverse, phase memory or spin–spin relaxation time, describes the loss of phase coherence by spin exchange between the individual protons. It is an isoenergetic process and reduces the lifetime of the alignment of a single magnetic moment parallel or antiparallel to the magnetic field, thus $T_2 \leq T_1$. Locally different fields or inhomogeneous media, i.e. media with different magnetic susceptibilities, can also be the source of a T_2 shortening; these effects are usually called T_2^* or susceptibility effects.

The magnetic relaxation times are influenced by various physical parameters, with the magnetic dipole–dipole interactions and their frequency spectrum being the most prominent ones. The relaxation times can be decreased further by magnetic substances. The efficiency by which these magnetic substances shorten the relaxation times are called relaxivities r_1 and r_2 according to

$$1/T_1 = 1/T_{10} + r_1 c \quad (1)$$

$$1/T_2 = 1/T_{20} + r_2 c \quad (2)$$

where $1/T_{10}$ and $1/T_{20}$ are the relaxation rates for the solvent/solution or plasma in the absence of the magnetic molecules and c (mol l^{-1}) is the concentration of the magnetic molecules. For paramagnetic substances the shortening of the relaxation times can be understood on the basis of the Solomon–Bloembergen equations.[23]

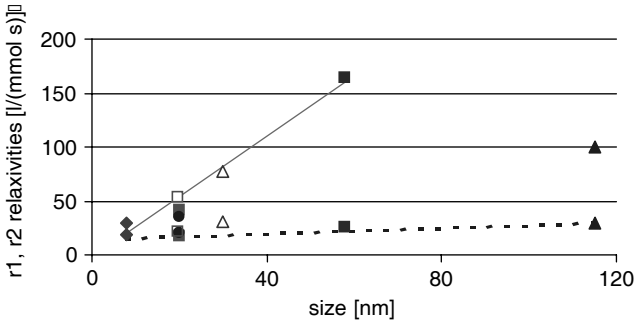

Figure 2. r_1 and r_2 relaxivity values as a function of particle size for VSOP[5] (filled diamond), USPIO[25] (SH U555C, gray filled square, Supravist®), USPIO[26] (AMI-227, open triangle, Sinerem®, Combidex®), USPIO[27] (NC100 150, filled circle, Clariscan®), SPIO[17] (SH U555A, filled square Resovist®), SPIO[28] (AMI-25, filled triangle Feridex®, Endorem®), USPIO[29] (open square); 37 °C, 0.47 T.

For the experimental determination of r_1 and r_2 the relaxation rates $1/T_1$ and $1/T_2$ are measured as a function of the concentration. Often these measurements are performed at a magnetic permeability $B = 0.47$ T. Though physically different from dissolved paramagnetic molecules like gadolinium diethylenetriaminepentaacetate, straight lines are obtained by plotting the measured relaxation rates $1/T_1$ and $1/T_2$ versus the concentration of the particles, i.e. the iron concentration in the present case. In a few cases r_1 and r_2 values were determined as a function of the applied magnetic permeability.[24] These measurements serve to understand the physical mechanism underlying the relaxation phenomena and are further helpful for choosing optimal parameters of the MRI pulse sequences.

A number of relaxivity values are plotted in Fig. 2 as a function of the particle size for both T_1 and T_2 at 0.47 T. With the exception of the r_2 of Feridex® (AMI-25), the relaxivities seem to fall on straight lines, with a linear increase in the relaxivity values with increasing particle size for both T_1 and T_2. With smooth transition, particles with diameter >30 nm are called SPIOs, and those with diameter <30 nm USPIOs.

MRI SIGNAL INTENSITIES

For standard spin echo pulse sequences with repetition time T_R and spin echo time T_E the MRI signal intensity SI is given by

$$SI = \rho(H) \exp(-T_E/T_2)[1 - \exp(-T_R/T_1)] \quad (3)$$

where $\rho(H)$ is the local proton density. If the relaxation rates $1/T_1$ and $1/T_2$ are inserted from Eqns (1) and (2) it follows that

for any chosen pair of T_E and T_R the SI becomes a function of the relaxivity values r_1 and r_2 and concentration c of the contrast medium.

$$\begin{aligned} SI &= \rho(H)\exp(-T_E/T_{20} - T_E r_2 c) \\ &\quad [1 - \exp(-T_R/T_{10} - T_R r_1 c)] \\ &= \rho(H)\exp(-T_E/T_{20})\exp(-T_E r_2 c) \\ &\quad [1 - \exp(-T_R/T_{10})\exp(-T_R r_1 c)] \end{aligned} \quad (4)$$

For fast low-angle shot (FLASH) sequences the flip angle θ is introduced and Eqn (3) has to be modified:

$$SI = \frac{\rho(H)\exp(-T_E/T_2)[1 - \sin(\theta)\exp(-T_R/T_1)]}{1 - \cos(\theta)\exp(-T_R/T_1)} \quad (5)$$

For $\theta = 90°$ Eqn (5) reduces to Eqn (3).

Common values for SPIOs are around 20 l mmol^{-1} s^{-1} and 160 l mmol^{-1} s^{-1} for the r_1 and r_2 relaxivities respectively and for USPIOs 20 l mmol^{-1} s^{-1} and 60 l mmol^{-1} s^{-1} respectively, at 0.47 T (see Fig. 2).

The intensities are calculated for two cases relevant to the clinical application of magnetic iron oxide particles. In Fig. 3a the signal intensities are calculated for parameters typically used in liver imaging; in Fig. 3b the signal intensities refer to fast sequences used for MR angiography.

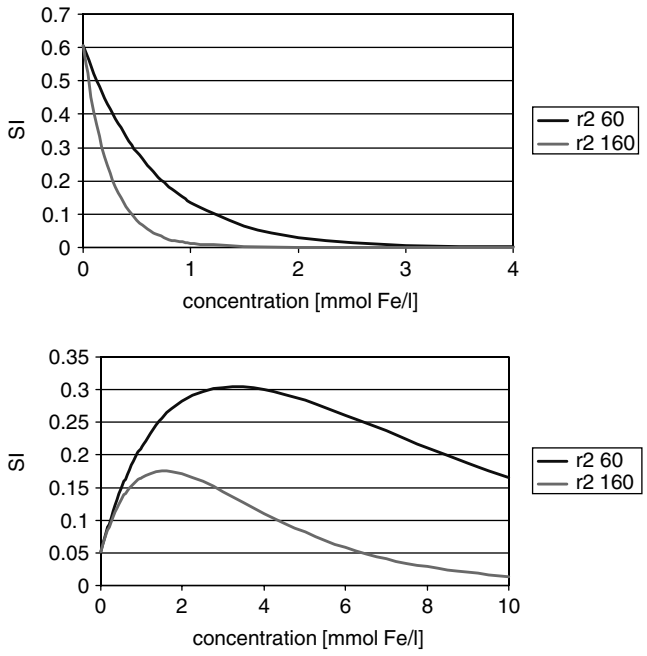

Figure 3. Calculation of signal intensities SI as a function of the concentration of the magnetic particles for liver imaging (top) and MR coronary angiography (bottom) with $r_1 = 20$ l mmol^{-1} s^{-1} and $r_2 = 60$ and 160 l mmol^{-1} s^{-1}, $\rho(H) = 1$.

Two conclusions can be drawn from Fig. 3: in liver imaging, even very low concentrations of the magnetic particles lead to a decrease of the signal intensity for both the SPIO and USPIO particles, with the larger particles being more effective. Thus, the signal intensity of liver locations at even low concentrations of the magnetic particles are dramatically reduced. In contrast to liver imaging, time-saving sequences with very short T_E and T_R and flip angles <90° are used in MR angiography. In the absence of magnetic particles the native signal intensity is low and increases with increasing concentration of the magnetic particles to a maximum value. Depending on the actual parameters, the signal intensity can reach a broad maximum before it starts to decline upon further increase in the concentration. The effect is more pronounced for the USPIO particles than for the SPIO particles. Consequently, vessels with the appropriate concentration of the magnetic particles in the bloodstream show an increase in signal intensity on the background of the surrounding tissue of low signal intensity. The situation is similar for other pulse sequences.

PHYSIOLOGICAL FATE OF SPIO AND USPIO PARTICLES

It is generally accepted that larger particles are preferentially taken up by macrophages in liver, spleen and bone marrow or lymph nodes. The mechanism is phagocytosis.[30] SPIOs, owing to their larger size, are taken up more rapidly than the USPIO particles.[3,31] The different uptake rates endow the USPIOs with longer blood half-lifes; they can escape the phagocytosis in liver and spleen and can find other targets.

IN VIVO RESULTS

Results on clinically used iron oxides have been reviewed by Clément *et al*.[32] In an earlier review, Weissleder and Papisov[33] focused both on clinically available and on experimental iron oxides. More recent reviews are by Wang *et al*.[34] and Taupitz *et al*.[35]

RES imaging: liver and spleen

The clinical development of magnetic iron oxide particles dates back to 1987.[13,36] Primary targets were the detection of focal liver and spleen lesions. SPIOs are rapidly cleared from the blood by the mononuclear phagocytosing system (MPS) in liver and spleen. This accumulation leads to a decrease in signal intensity of normal parenchyma, especially in T_2-weighted images. Focal liver lesions without an MPS or without an intact MPS (called Kupffer cells in the liver) do not show this accumulation and maintain their pre-contrast signal intensity. Thus, SPIO-enhanced MRI shows an increase of liver-to-tumor contrast with respect to the pre-contrast images. Figure 4 presents one characteristic example.

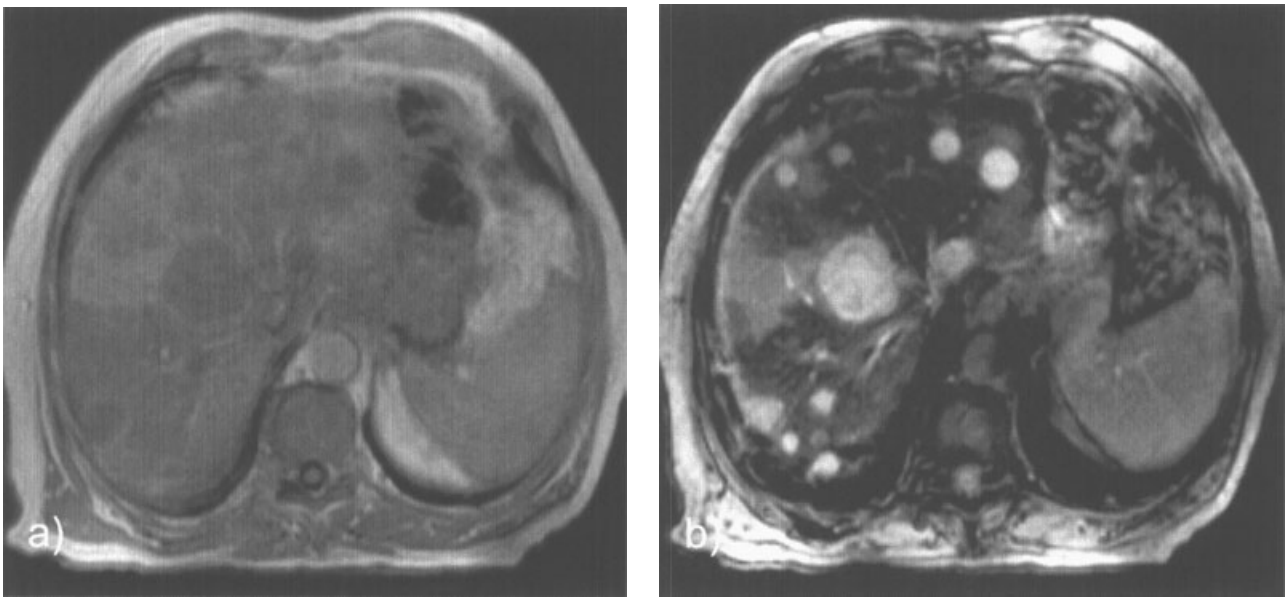

Figure 4. Liver MR images. Metastases of a gall bladder carcinoma. Left: shortly after the application of Resovist®; dynamic phase T_1-weighted two-dimensional FLASH image. Right: accumulation phase, T_2-weighted two-dimensional FLASH. 10 μmol of iron per kilogram body weight. A number of metastases are clearly seen, especially in the T_2-weighted image. For details see Reimer and Tombach.[38] (Courtesy of Dr B. Tombach, Department of Radiology, University Hospital Münster, Germany).

The specific advantages of the two substances clinically available for the demarcation of liver tumors, and their diagnostic values for the differential diagnosis of malign versus benign liver lesions or metastases, are discussed in the radiological literature and are recently reviewed by Wang *et al*.[34] and Taupitz *et al*.[35]

One way to perform volume-selective MR spectroscopy of tumors or metastases relies on the accumulation of iron oxide particles by the Kupffer cells of the liver. This leads to a signal reduction in the healthy liver; the parts infiltrated by tumors and metastases are not influenced. Consequently, MR spectra of the tumor can be obtained without volume-selective MR sequences, as probed by Römer *et al*.[37] The method should allow the monitoring of tumor therapy.

Although the MPS in liver and spleen adds only a few percent to the total organ mass or volume, even low local SPIO concentrations, due to the high magnetic efficiency, still lead to remarkable signal loss in liver and spleen. The iron oxide particles are taken up by the macrophages very efficiently and concentrated intracellularly in organelles. In these organelles the iron particles are broken down and, with a delay of a few days, the iron is fed into the body iron pool, e.g. it is incorporated into the hemoglobin of the red blood cells.[17]

Since liver and spleen constitute a large sink for SPIOs, their blood half-life of SPIOs is only a few minutes. For the targeting of other organs, e.g. lymph nodes, blood vessels or distant tumors, the longer blood half-life of 1–2 h is advantageous for the USPIOs.

MR LYMPHOGRAPHY USING IRON OXIDE PARTICLES

Lymph nodes are of critical importance in the staging and prognosis of solid tumors. MRI with USPIOs is in clinical development for assessing lymph node status. Convincing results with high-resolution MRI after administration of magnetic nanoparticles were recently reported on the detection of small and otherwise undetectable lymph node metastases in patients with prostate cancer.[39] Two ways of accumulation are discussed. In the first, USPIOs use a transcapillary passage through the venules to reach the sinuses within the lymph nodes, where the USPIOs are taken up by phagocytosis. The second pathway occurs by transcytosis into the interstitial space followed by a draining to the lymphatic vessels and transport to the regional lymph nodes via afferent lymphatic channels. The problem has been addressed by Mühler *et al*.[29] Independent of the mechanism, the USPIO particles are taken up by macrophages, thus leading to a decrease of signal intensity of the healthy tissue while metastases are spared from this uptake mechanism with no change of signal intensity.

MR angiography

As can be seen from Fig. 3, an increase in signal intensity is obtained upon administration of iron oxide particles in MR angiography. USPIOs are administered for two favorable reasons: (1) the increase of the signal intensity over the background is more pronounced for USPIOs

than for SPIOs; (2) USPIOs have a longer blood half-life, so that both the bolus tracking phase and a quasi-stationary phase are available. Slightly higher doses of around 40–50 μmol of iron per kilogram, compared with about 10 μmol of iron per kilogram for liver imaging, have to be administered. Four different USPIOs are currently being studied in clinical trials and compete with blood-pool agents composed of gadolinium-chelates for the same or very similar indications.

Figure 5 shows one example. The substance is administered intravenously. In Fig. 5a the bolus tracking phase is seen; this is an early phase where the USPIOs reside almost exclusively in the arteries. At a later equilibrium phase the USPIOs are equally distributed over arteries and veins and, therefore, more diluted, with a concomitant decrease in signal intensity.

FUTURE INDICATIONS: LABELING OF MAMMALIAN CELLS

Mammalian progenitor or stem-cell therapy is currently being discussed for use against an increasing number of diseases. SPIOs have been used to label these cells, e.g. *ex vivo*,[41] providing future possibilities to monitor the cell migration and proliferation by MRI non-invasively.

The covalent binding of proteins, antibodies or other target molecules to the coating of SPIOs is a powerful method of magnetically addressing and labeling cells *in vivo* to study their biodistribution non-invasively. Examples are the labeling of oligodendrocyte precursor cells which have potential value of repair in demyelinated lesions like multiple sclerosis,[42] the detection of apoptosis[43] and the molecular imaging of breast cancer cells.[44]

CONCLUSIONS

A variety of analytical techniques are necessary to characterize the magnetic iron oxides used as contrast agents in MRI. Two particle ensembles have proven to be of diagnostic benefit i.e. SPIOs and USPIOs. SPIOs, with hydrodynamic diameter >30 nm, are taken up by stationary macrophages in liver and spleen, leading to a pronounced signal loss in these tissues. In many cases metastases and cancers are devoid of this uptake mechanism. After administration of SPIOs, the contrast between tumor and healthy tissue is increased due to the uptake of the magnetic particles by the healthy but not by the tumorous tissue. The USPIOs (<30 nm diameter) can escape the initial uptake by liver and spleen, they can reach other targets and can serve as a blood pool agent. If short pulse sequences are used the lower r_2 of these smaller particles can lead to pronounced increases in signal intensities which are helpful for the demarcation of arteries and veins.

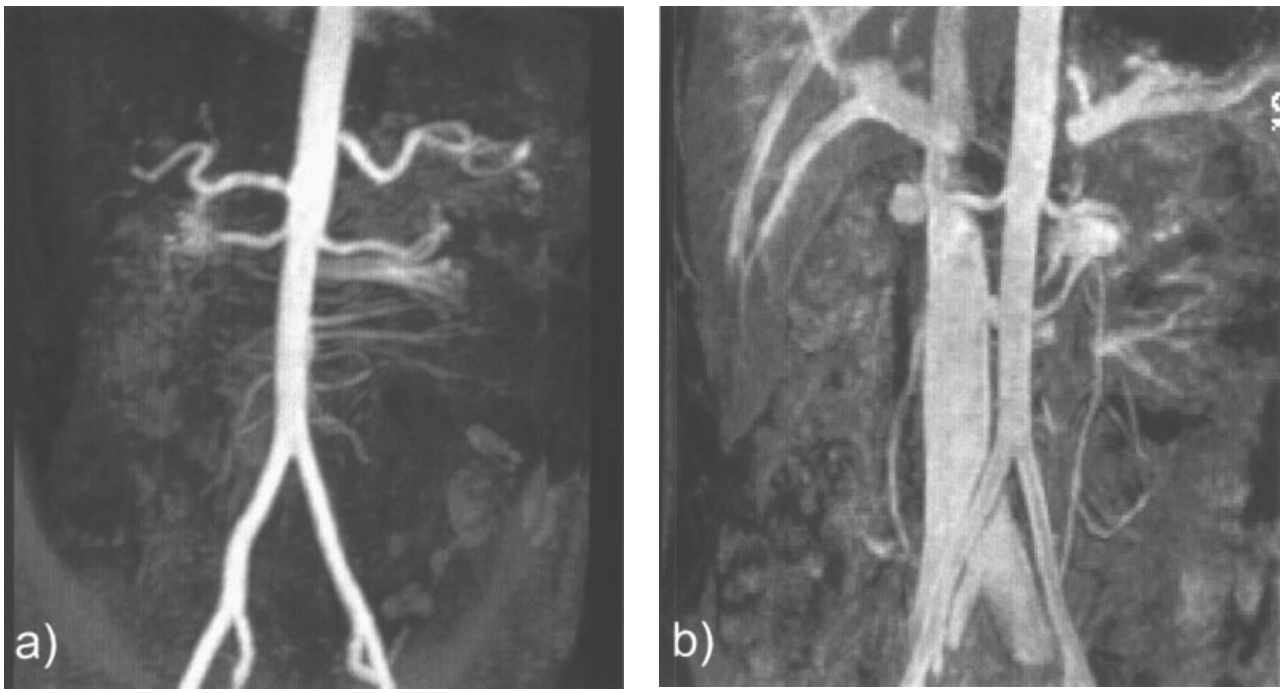

Figure 5. Contrast-enhanced MR angiography (three-dimensional FLASH) after i.v. injection of Supravist® at a dose of 40 μmol of iron per kilogram body weight. (a) First-pass arterial phase (11 s post-injection). (b) Steady-state phase (20 min post-injection) showing the enhancement of both arteries and veins. For details see Tombach *et al*.[40] (Courtesy of Dr B. Tombach, Department of Radiology, University Hospital Münster, Germany).

SPIOs and USPIOs are considered as T_2 relaxation agents with $r_2 > r_1$, in contrast to the molecularly dissolved and hydrophilic paramagnetic gadolinium complexes with $r_2 \approx r_1$.

Iron oxide particles are taken up by macrophages and, with a time delay, incorporated into the endogeneous iron pool. Normal diagnostic doses increase this iron pool by a few percent only.

Magnetic iron oxide particles are discussed with respect to the *in vivo* monitoring of cell migrations and as a tool for molecular and functional MRI.

REFERENCES

1. Fahlvik AK, Klaveness J, Stark DD. *J. Magn. Reson. Imaging* 1993; **3**: 187.
2. Häfeli U. The mystery and history of magnetism. In *Scientific and Clinical Applications of Magnetic Carriers*, Häfeli U, Schütt W, Teller J, Zborowski M (eds). Plenum Press: New York, 1997; 1–10.
3. Weissleder R, Elizondo G, Wittenberg J, Rabito CA, Bengele HH, Josephson L. *Radiology* 1990; **175**: 489.
4. Taupitz M, Schnorr J, Abramjuk C, Wager S, Pilgrimm H, Hunigen H, Hamm B. *J. Magn. Reson. Imaging* 2000; **12**: 905.
5. Wagner S, Schnorr J, Pilgrimm H, Hamm B, Taupitz M. *Invest. Radiol.* 2002; **37**: 167.
6. Hahn PE, Stark DD, Lewis JM, Saini S, Elizondo G, Weissleder R, Fretz CJ, Ferrucci JT. *Radiology* 1990; **175**: 695.
7. Jacobsen TF, Laniado M, VanBeers BE, Dupas B, Boudghene FP, Rummeny E, Falke H, Rinck PA, MacVicar D, Lundby B. *Acad. Radiol.* 1996; **3**: 571.
8. Shen T, Weissleder R, Papisov M, Bogdanov A, Brady TJ. *Magn. Reson. Med.* 1993; **29**: 599.
9. Molday R, Mackenzie D. *J. Immunol. Methods* 1982; **52**: 353.
10. Ohgushi M, Nagayama K , Wada A. *J. Magn. Reson.* 1978; **29**: 599.
11. Hasegawa M, Hokkoku S. US Patent No. 4101435, 18 July 1978.
12. Seneterre E, Weissleder R, Jaramillo D, Reimer P, Lee AS, Brady TJ, Wittenberg J. *Radiology* 1991; **179**: 529.
13. Saini S, Stark DD, Hahn PF, Wittenberg J, Brady TJ, Ferrucci JT. *Radiology* 1987; **162**: 211.
14. Kreft BP, Tanimoto A, Leffler S, Finn JP, Osendal AN, Stark DD. *J. Magn. Reson. Imaging* 1994; **4**: 373.
15. Weissleder R, Reimer P, Lee AS, Wittenberg J, Brady TJ. *Am. J. Roentgenol.* 1990; **155**: 1161.
16. Pfefferer D. Synthese, *in-vitro-* und *in-vivo*-Charakterisierung von Chondroitin-4-sulfat-stabilisierten superparamagnetischen Eisenoxiden und ihre Anwendung als Kontrastmittel für die Magnetische-Resonanz-Tomographie. Ph.D. thesis, Department of Pharmacy, Freie Universität Berlin, 1993.
17. Lawaczeck R, Bauer H, Frenzel T, Hasegawa M, Ito Y, Kito K, Miwa N, Tsutsui H, Vogler H, Weinmann HJ. *Acta Radiol.* 1997; **38**: 584.
18. Dutton A, Tokuyasu K, Singer S. *Proc. Natl. Acad. Sci. U.S.A.* 1979; **76**: 3392.
19. Kresse M, Wagner S, Pfefferer D, Lawaczeck R, Elste V, Semmler W. *Magn. Reson. Med.* 1998; **40**: 236.
20. Cerdan S, Lötscher HR, Künnecke B, Seelig J. *Magn. Reson. Med.* 1989; **12**: 151.
21. Wunderbaldinger P, Josephson L, Weissleder R. *Acad. Radiol.* 2002; **9**: (Suppl. 2): S304.
22. Prene P, Tronc E, Jolivet JP, Dormann JL. Mössbauer spectra of γ-Fe_2O_3 nanoparticles. In *ICAME-95. Conference Proceedings* 1996; vol. 50; 485.
23. Wesbey GE. Magnetopharmaceuticals. In *Biomedical Magnetic Resonance Imaging. Principles, Methodology, and Applications*, Wehrli FW, Shaw D, Kneeland JB, (eds). VCH Verlagsgesellschaft: Weinheim, 1988.
24. Bulte JWM, Vymazal J, Brooks RA, Pierpoali C, Frank JA. *J. Magn. Reson. Imaging* 1993; **3**: 641.
25. Knollmann FD, Bock JC, Rautenberg K, Beier J, Ebert W, Felix R. *Invest. Radiol.* 1998; **33**: 637.
26. Tanimoto A, Yuasa Y, Hiramatsu K. *J. Magn. Reson. Imaging* 1998; **8**: 446.
27. Saeed M, Wendland MF, Engelbrecht M, Sakuma H, Higgins CB. *Eur. Radiol.* 1998; **8**: 1047.
28. Jung CW, Jacobs P. *Magn. Reson. Imaging* 1995; **13**: 661.
29. Mühler A, Zhang X, Wang H, Lawaczeck R, Weinmann HJ. *Invest. Radiol.* 1995; **30**: 98.
30. Pratten MK, Lloyd JB. *Biochim. Biophys. Acta* 1986; **881**: 307.
31. Bowen CV, Zhang X, Saab G, Gareau PJ, Rutt BK. *Magn. Reson. Med.* 2002; **48**: 52.
32. Clément O, Siauve N, Cuénod C-A, Frija G. *Top. Magn. Reson. Imaging* 1998; **9**: 167.
33. Weissleder R, Papisov M. *Rev. Magn. Reson. Imaging* 1992; **4**: 1.
34. Wang Y-XJ, Hussain SM, Krestin GP. *Eur. Radiol.* 2001; **11**: 2319.
35. Taupitz M, Schmitz S, Hamm, B. *Fortschr. Röntgenstr.* 2003; **175**: 752.
36. Stark DD, Weissleder R, Elizondo G, Hahn PF, Saini S, Todd LE, Wittenberg J, Ferrucci JT. *Radiology* 1988; **168**: 297.
37. Römer T, Gewiese B, Stiller D, Plötz M, Lawaczeck R, Wolf KJ. *Fortschr. Röntgenstr.* 1990; **153**: 79.
38. Reimer P, Tombach B. *Eur. Radiol.* 1998; **8**: 1198.
39. Harisinghani MG, Barentsz J, Hahn PF, Deserno WM, Tabatabaei S, van de Kaa CH, de la Rosette J, Weissleder R. *New Engl. J. Med.* 2003; **348**: 2491.
40. Tombach B, Reimer P, Mahler M, Ebert W, Pering C, Heindel W. *Acad. Radiol.* 2002; **2**(9): S425.
41. Frank JA, Zywicke H, Jordan EK, Mitchell J, Lewis BK, Miller B, Bryant H, Bulte JWM. *Acad. Radiol.* 2002; **9**: S484.
42. Franklin RJ, Blaschuk KL, Bearchell MC, Prestoz LL, Setzu A, Brindle KM, French-Constant C. *Neuroreport* 1999; **10**: 3961.
43. Zhao M, Beauregard DA, Loizou L, Davletov B, Brindle KM. *Nat. Med.* 2001; **7**: 1241.
44. Artemov D, Mori N, Okollie B, Bhujwalla ZM. *Magn. Reson. Med.* 2003; **49**: 403.